# SOME MODELS OF NEURONAL VARIABILITY

R. B. STEIN

*From the University Laboratory of Physiology, Oxford, England*

ABSTRACT The pattern of nerve action potentials produced by unit permeability changes (quantal inputs) occurring at random is considered analytically and by computer simulation methods. The important parameters of a quantal input are size and duration. Varying both the mean and the probability density function of these parameters has calculable effects on the distribution of interspike intervals. Particular attention is paid to the relation between the mean rate of excitatory inputs and the mean frequency of nerve action potentials (input-output curve) and the relation between the coefficient of variation for the interval distribution and the mean interval (variability curve). In the absence of action potentials one can determine the parameters of the voltage distribution including the autocorrelation function and the power spectrum. These parameters can sometimes be used to approximate the variability of interspike intervals as a function of the threshold voltage. Different neuronal models are considered including one containing the Hodgkin-Huxley membrane equations. The negative feedback inherent in the Hodgkin-Huxley equations tends to produce a small negative serial correlation between successive intervals. The results are discussed in relation to the interpretation of experimental results.

## INTRODUCTION

Adrian and Zotterman (1926) first showed that single nerve cells often code the intensity of sensory stimuli as a frequency of action potentials in a long train. Variability in the intervals between successive nerve impulses has often been looked upon as unwanted "noise," since, with fluctuations present, one must average over a number of impulses to measure the mean frequency accurately. However, neuronal variability has been attracting a growing amount of attention for three main reasons:

1. If the frequency of nerve impulses conveys information about stimulus intensity to the central nervous system, the variability limits, not only the accuracy of an experimenter's determination of mean frequency, but also the amount of information a nerve cell can transmit about its environment.
2. In addition to information contained in the mean frequency, the exact timing of nerve impulses is sometimes important (Barlow, 1963), so one must study the whole impulse pattern.
3. Where intracellular recording is impossible, the sequence of nerve impulses may be the only available data. What do the fluctuations in interval indicate about the mechanism of nerve impulse generation?

This paper deals with this last problem by considering simplified models and deriving their statistical properties. By analyzing various models based on different experimental results, one can begin to associate certain phenomena and certain mechanisms with impulse patterns or other statistical quantities. Generally, no unique solution exists; any number of mechanisms could generate a given pattern. However, the range of common physiological phenomena severely limits the range of possible mechanisms. In particular, the mechanisms will often be based on permeability changes to one or more ions.

I shall assume that the variability arises from the random occurrence of unit permeability changes. Much work in this field has started from another assumption, namely that there is a source of Gaussian noise added to an otherwise determinate neuronal model. The thermal noise associated with the resistance of the membrane is a Gaussian noise source, but even in isolated axons thermal noise cannot account for the amplitude (Verveen, 1962) or the frequency spectrum (Verveen and Derksen, 1965) of observed fluctuations in excitability and membrane voltage. These fluctuations may result from the opening and closing of single permeability channels or pores in the membrane (Derksen, 1965). In some receptors, e.g. visual receptors (Adolph, 1964), and at synapses much larger unitary permeability changes occur, associated with the spontaneous release of single packets of transmitter or the discharge of a presynaptic nerve fiber.

Models based on the discrete nature of the permeability changes will be called "quantal" models to distinguish them from Gaussian noise models. The term "quantum" or "quantal input" will indicate a unit permeability change,[1] whether it arises from the absorption of a light quantum by a photoreceptor, the release of a packet of transmitter at a synapse, or the opening of a single membrane pore. Even if different sized inputs are present together, one can make predictions from the unit events. Only if the size of all inputs is small and the rate of occurrence high will the predictions of Gaussian noise and quantal models agree (Geisler and Goldberg, 1966).

To predict neuronal variability, assumptions are also required about the behavior of the nerve cell in the absence of variability (the average time and voltage dependence of the membrane properties). Previous work on variability (see Moore, Perkel, and Segundo, 1965, for a review) assumed "classical" neuronal properties. Models consisted of a linear current-voltage curve with a sharply defined threshold voltage, although in some models the threshold varied with time due to accommodation of the Hill type (Hill, 1936) or the various phases of excitability that follow a nerve impulse. I shall follow this tradition initially to extend previous work, but will later consider a model based on the full Hodgkin-Huxley equations.

At a given time after a brief suprathreshold stimulus, one can determine the

[1] Stein (1965) used the term "impulse" synonomously with quantal input, but this may be confused with the nerve impulse or action potential and so will not be used here.

threshold voltage to which the nerve membrane potential must be raised just to elicit a second nerve impulse. A threshold voltage may not exist for a certain time (absolute refractory period). It generally has a higher than normal value at some later times (relative refractory period), but gradually returns toward its quiescent value. Similarly, unless the membrane is spontaneously active, the membrane potential will return to its quiescent value, generally with one or more oscillations.

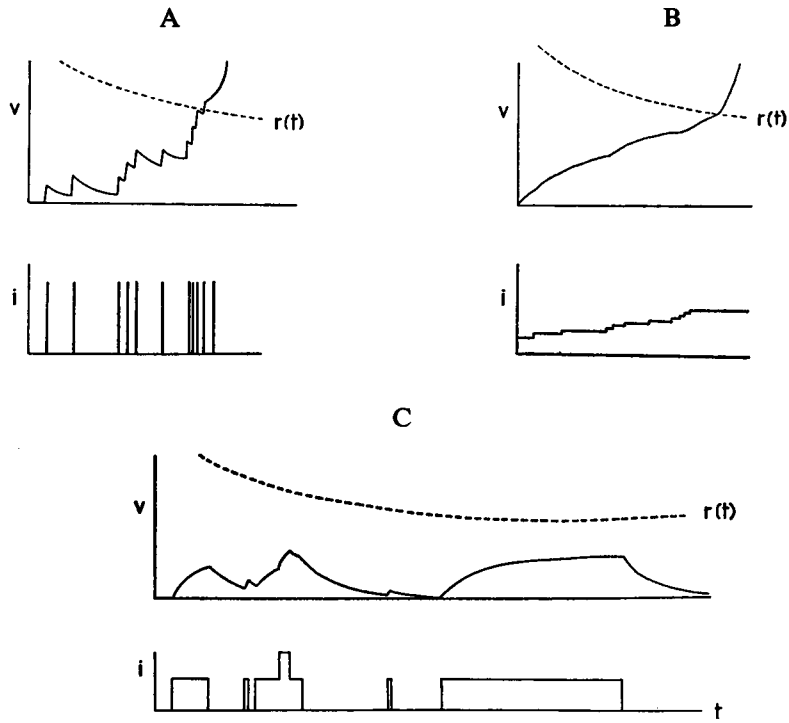


FIGURE 1 Schematic representation of some models of neuronal variability. With a short acting transmitter (A) the random current inputs produce characteristic unit voltage changes which sum to reach a threshold level, $r(t)$. If the permeability changes produce longer, weaker currents (B), the voltage changes more smoothly. Some current remains from before the previous action potential ($t < 0$). The currents produced by single pores opening and closing (C) may also have variable duration.

An added quantal input, such as the release of a packet of transmitter at a synapse, produces an extra voltage, which often decays approximately exponentially (with time constant $\tau$) after the end of the permeability change. Fig. 1A shows a random series (Poisson process) of quantal inputs on a transformed plot. The voltage $v$ is the *extra* voltage change at any time and is reset to zero after each nerve impulse. $r(t)$ is the extra voltage change required to reach threshold at a given time ($t$) after the first stimulus and thus includes changes in threshold and some effects of after-potentials. This transformation is only strictly valid if the current-voltage curve is

linear and independent of time, e.g., the conductance changes associated with the afterpotentials are neglected. Also neglected is the decrease in the voltage change produced by unit permeability changes as the excitatory equilibrium potential is approached (Martin and Pilar, 1964).

In Fig. 1A the quantal inputs, e.g. synaptic currents, were large, though short-lasting. A smaller quantal input of longer duration could produce roughly the same time to reach threshold (Fig. 1B). However, the voltage changes are smoother and the discharge pattern of the cell is rather different. The average rate of quantal inputs will be denoted $p_e$ and their duration $t_p$ ; both parameters are assumed to be voltage independent. Fig. 1 shows rectangular current inputs for convenience since the magnitude and duration are then clearly defined and the rise time of the voltage change (time to peak) is also $t_p$ . If the quantal inputs are derived from a Poisson process, the probability of an input in a short time $\delta t$ is $p_e \delta t$, and the average number active at any one time is $p_e t_p$ .

These detailed assumptions may seem restrictive, but the predictions of these simplified models are more easily obtained analytically and provide a useful basis for comparison. Later sections consider more realistic models with quanta of variable size and shape and non-Poisson inputs.

## NOTATION

The rapid growth of the subject of neuronal models has produced a large number of new terms. I shall use wherever possible the same symbols as Moore et al. (1965) in their review article. The main symbols used in this paper are:

$V(t)$, the extra voltage at a time $t$ after a nerve impulse resulting from quantal permeability changes.

$f(v, t)$, the probability that $V(t) = v$ at time $t$ assuming $V(0) = 0$. The mean voltage level as a function of time is denoted $\mu_v \equiv \int v f(v, t)\, dv$ and the variance in voltage level is denoted $\sigma_v^2 \equiv \int (v - \mu_v)^2 f(v, t)\, dv$. The autocovariance function $\gamma(h)$, the autocorrelation function $\rho(h)$, and the power spectrum $P(\omega)$ will be introduced later.

$_1(t)$, the *interval density* function (Gerstein and Kiang, 1960), is the probability that the voltage just reaches threshold at time $t$ after the last impulse. I shall sometimes indicate that the voltage started at a level $v$ and reached a level $r$ by using the form $f_{v,r}(t)$. In the statistical literature, $f(t)$ would be the probability density function of first passage times to an absorbing barrier. The following are important parameters of the interval density function and will be used without subscripts: the mean interval, $\mu$; the variance of the interval density function, $\sigma^2$; the coefficient of variation, $\sigma/\mu$; and the mean frequency of nerve impulses, $\nu = 1/\mu$.

$F(t) = \int_0^t f(t)\, dt$, the corresponding probability distribution function, will be called the *interval distribution* function. It measures the cumulative probability of the voltage reaching threshold at a time *less than or equal to* $t$. Both the interval density function and the interval distribution can be estimated from an experimental interval histogram. The interval distribution is often more useful for comparing different experimental results or experiment with theory since it always increases from zero to one as $t$ changes from zero to $\infty$. Standard nonparametric statistical tests for the homogeneity of different experimental samples or for the significance of deviations of experiment from theory (Fisz, 1963, section 10.11) can then be applied.

$\varphi(t) = f(t)/[1 - F(t)]$; $\varphi(t)\delta t$ is the conditional probability that a nerve impulse will occur between the times $t$ and $t + \delta t$, given that an impulse has not occurred by time $t$. Several names have been used for this function (see Moore *et al.*, 1965, p. 497) including the term *conditional probability* function (Goldberg, Adrian, and Smith, 1964). If the duration of significant correlations in voltage level is short, $\varphi(t)$ will contain information about the recovery process governing the excitability of the cell after a nerve impulse. Therefore, the peaks and troughs of this function (Poggio and Viernstein, 1964) may be more important than those of the interval histogram. When the interval density function is exponential, $\varphi(t)$ is a constant equal to the mean frequency of nerve impulses. I shall sometime plot $\ln [1 - F(t)]$ against $t$, (see also Smith and Smith, 1965) since the slope is

$$\frac{d}{dt}\{\ln [1 - F(t)]\} = \frac{d[-F(t)]/dt}{1 - F(t)} = \frac{-f(t)}{1 - F(t)} = -\varphi(t).$$

One can often determine $\varphi(t)$ from small samples in this way, when a direct plot would show considerable scatter.

More general input processes are considered in later sections. The mean voltage produced by a quantal input at a time $u$ after its occurrence will be some arbitrary function $g(u)$. $q(a)$ will denote the amplitude density function of single voltage changes with mean $\mathbf{a}$ and second moment $\mathbf{a}^2 = \int a^2 q(a)\, da$. Also the probability that the next quantal input occurs at a time $u$ after the last input will be a function $b(u)$. The mean time will be $1/p$ where $p$ is the mean rate of quantal inputs (both excitatory and inhibitory) and the variance in time will be denoted $\sigma_p^2$. Finally I shall consider the probability density function of stimulus current, relative to the current produced by a unit permeability change. This density function will be called $y(i)$ with mean $\mu_i$ and variance $\sigma_i^2$.

Much of the work will center around two relationships, the "input-output curve" relating the mean impulse frequency, $\nu$, to the rate of excitatory inputs, $p_e$, and the "variability curve" relating the coefficient of variation, $\sigma/\mu$, of the interval distribution to the mean interval.

## RESULTS

### 1. *Short-Duration Inputs*

Let the duration of the currents produced by quantal inputs be much less than the membrane time constant $\tau$ and the average number active at any time be much less than the threshold number. The reasons for the second assumption will become clear in a later section (Longer Duration Inputs). The rise time of the voltage changes will then be short and the exponential shape of the voltage change will be little affected by the precise quantal shape or duration. Since a linear system has been assumed initially, the peak voltage produced by a quantal input can be set equal to one without loss of generality, i.e., voltage will be measured in multiples of the extra voltage produced by a single quantum. This rather simple model will be called the *exponential decay model*; its assumptions are summarized in Table I, and Table II lists some results derived (Stein, 1965) for a constant threshold $r$. Computer simulation studies can extend these analytical results and I shall consider briefly two further properties of this model, its input-output characteristics and its relative variability.

*Input-Output Relation.* In the absence of variability the frequency of nerve impulses produced by constant current stimuli (frequency-current curve) was considered (Stein, 1967) for a number of models. This curve was generally only linear over a limited middle range of impulse frequencies with negative deviations from linearity at both high frequencies and low frequencies. The deviations at high frequencies were due to refractory effects which will be considered later. The solid line on the right of Fig. 2 shows the predicted deviation at low frequencies (neglecting accommodation and the effects of a supernormal period of excitability). To compare different conditions, $\nu$ is multiplied by the time constant $\tau$ and stimulus strength is divided by the threshold value to give a dimensionless plot. A constant

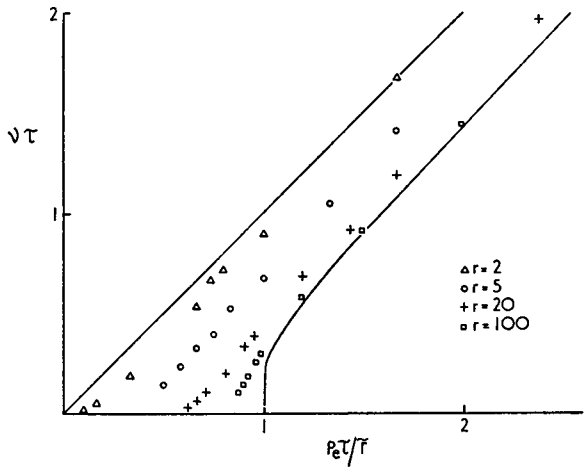


FIGURE 2 Input-output relation for the exponential decay model. The mean frequency of nerve impulses ($\nu$) and the rate of quantal permeability changes $p_e$ were multiplied by the membrane time constant $\tau$, to give a dimensionless plot. $p_e$ was also divided by the minimum number of quanta required to reach threshold so that different threshold levels ($r$) can be readily compared.

current can be considered to result from a negligibly small quantal size and impulse initiation will then just occur (Stein, 1965) when $p_e\tau = r$. Hence, stimulus strength is indicated as the ratio $p_e\tau/\bar{r}$ in Fig. 2.

With decay present, the next integral number of quanta beyond threshold must occur before an impulse is initiated. With $r = 2$, or say 2.8, at least $\bar{r}$ = integral part of $r + 1$ = 3 quanta are needed.

The solid line on the left is the opposite extreme where every unit event produces a nerve impulse ($r \leq 1$). The data points are simulated results for intermediate values of the threshold $r$. Two effects of the random input are apparent: the input-output relationship is more linear than that obtained with constant current stimuli

and the apparent threshold is reduced. Both these effects may be important, for example, in preserving low-level intensity information in a multisynaptic afferent pathway.

*Coefficient of Variation.* A useful quantity in discussing the relative variability of nerve discharges is the coefficient of variation ($\sigma/\mu$) for the interval distribution and Table II gives its values in the limits $\mu \ll \tau$ and $\mu \gg \tau$. Intermediate values are not easily calculable analytically except by an approximate method which is described later and is only accurate for large $r$ when $\sigma < \tau/4$. The data points of Fig. 3 show a wide range of values determined by computer simulation as described

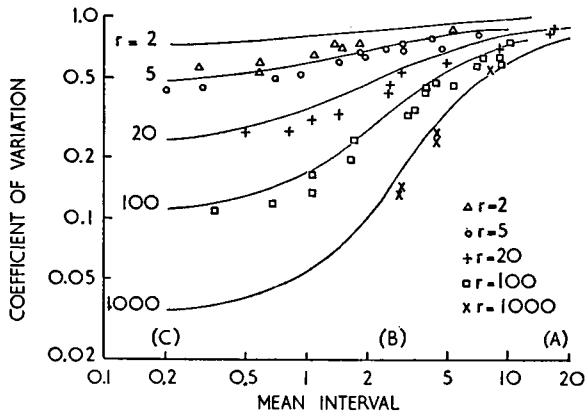


FIGURE 3 Variability curve for the exponential decay model (data points) and the variable duration model (solid curves). The threshold levels ($r$) are indicated by the key on the right for the exponential decay model and by the numbers to the left of the solid curves for the exponential decay model. Log-log scale; mean interval in multiples of the time constant $\tau$.

previously (Stein, 1965) for thresholds from $r = 2$ to $r = 1000$. This log-log plot of coefficient of variation against mean shows three distinct regions, labeled (*A*), (*B*), and (*C*) in Fig. 3. At long mean intervals, the coefficient of variation approaches one (the characteristic of an exponential density function) irrespective of the value of the threshold $r$. As the input rate is increased, the mean interval decreases (Fig. 3, region *B*) and the firing pattern becomes more regular until at very short intervals the coefficient of variation approaches a new constant value (region *C*).

The solid lines, calculated from a related (variable duration) model, suggest that on this scale the variability curve is sigmoid. However, the computer simulated points show a scatter similar to that of experimental data and can be usefully approximated by three straight line segments. The two regions of constant coefficient of variation (lines of zero slope at short and long mean intervals) are joined by a transition region in which the slope of the best-fitting line varies systematically as a function of the parameter $r$.

A straight line of a log-log scale would indicate that the coefficient of variation ($\sigma/\mu$) increased as a power function of the mean interval ($\mu$); the slope on this scale gives the exponent. If the model accurately describes the experimental situation, one can obtain estimates for the threshold $r$ and time constant $\tau$ by comparing experimental curves in milliseconds with simulated curves in time constants. Data from cat muscle spindle afferents (Stein and Matthews, 1965) and cat chemoreceptors (Silk and Stein, 1966) were analyzed in this way. Biederman-Thorson (1966) suggested that a gamma distribution model could not easily explain the common experimental finding (Verveen and Derksen, 1965) of a standard deviation increasing as the square of the mean interval, i.e., a coefficient of variation ($\sigma/\mu$) increasing linearly with mean. Her apparent "paradox" results from consideration only of asymptotic values (region *C*). The experimental mean intervals (tens or hundreds of milliseconds in duration) were presumably from a transition region (region *B*) where the power function exponent varies widely as a function of the threshold number $r$.

*Variable Duration.* Consider a model in which voltage changes are not exponential, but rectangular with a random duration of mean $\tau$. The reason for again using the symbol $\tau$ is that *on average* the voltage still decays exponentially with time constant $\tau$. Although rather more unrealistic, this *variable duration* model with its limited number $(r + 1)$ voltage levels offers certain analytical advantages. This same model applies to telephone exchanges, (Palm, 1943) assuming calls occur at random and have random durations, and to population statistics where it has been called an "immigration-death" process (Cox and Miller, 1965). Table II lists the limiting properties of the model. For strong stimuli ($p_e\tau \gg r$) the results approach those of the exponential decay model. For weak stimuli, the extra random feature of the variable duration model increases the chance of the voltage reaching threshold and hence increases the impulse frequency.

Iso (1965) showed that starting from a voltage $v$ the Laplace transform of first passage times (interval density function) to reach a voltage $r$ is

$$f^*_{v,r}(s) = p_e{}^{r-v} B_v(s)/B_r(s) \tag{1.1}$$

where $p_e$ is the mean rate of events per time constant $\tau$, $f^*_{v,r}(s) \equiv \int_0^\infty e^{-st} f_{v,r}(t)\, dt$, and $B_k(s)$ is a polynomial of $s$ in degree $k$. $B_0(s) = 1$, $B_1(s) = s + p_e$, and in general

$$B_k(s) = \sum_{j=0}^{k} \binom{k}{j} p_e{}^j s_{(k-j)}$$

where $\binom{k}{j}$ is a binomial coefficient and

$$s_{(m)} = s(s + 1) \cdots (s + m - 1) \quad \text{with} \quad s_{(0)} = 1.$$

Starting from $v = 0$, the mean interval in units of the time constant $\tau$ can be

obtained by differentiating equation (1.1) with respect to $s$ and evaluating at $s = 0$ (Fisz, 1963, p. 108).

$$\mu = \frac{-\partial f^*_{0,r}(s)}{\partial s}\bigg|_{s=0} = \frac{p_e{}^r B_r{}'(0)}{[B_r(0)]^2} = \sum_{j=0}^{r-1} \frac{r!}{j!} \frac{p_e{}^{j-r}}{(r-j)} \tag{1.2}$$

The variance can be similarly obtained.

$$\begin{aligned} \sigma^2 = \frac{\partial^2 f^*_{0,r}(s)}{\partial s^2}\bigg|_{s=0} - \mu^2 &= \frac{p_e{}^r\{2[B_r{}'(0)]^2 - B_r{}''(0)B_r(0)\}}{[B_r(0)]^3} - \mu^2 \\ &= \mu^2 - B_r{}''(0)/p_e{}^r = \mu^2 - \sum_{j=0}^{r-2} \frac{r!}{j!} \frac{p_e{}^{j-r}}{(r-j)} \sum_{k=1}^{r-j-1} \frac{2}{k} \end{aligned} \tag{1.3}$$

ten Hoopen (1966) using a different method obtained bulkier, though, I think, equivalent expressions to equations (1.2) and (1.3). Iso (1965) calculated some interval density functions and also the input-output relations corresponding to Fig. 2 for the exponential decay model. Not only are negative deviations from linearity in the input-output curve at low frequencies reduced, but positive deviations are also evident at very low frequencies. Including a refractory period would make the input-output relation sigmoid.

The solid lines in Fig. 3 are calculated variability curves for the variable duration model with the same values of threshold as in simulations of the exponential decay model. The extra source of variability (duration) increases the coefficient of variation somewhat at all mean intervals in the transition region, but the major effect is simply to shift the variability curve to the left. In other words, introducing an exponentially distributed mean duration reduces the apparent value of the time constant $\tau$, since the mean interval in Fig. 3 is measured in units of the time constant $\tau$.

The smallest quantal numbers show an additional effect since $\bar{r}$ = integral part of $r + 1$ quanta must occur to reach threshold in the exponential decay model. With exponential decay and $r = 2$, at least three unit excitations must occur while in the variable duration model two quanta suffice. The variability at short intervals is reduced accordingly in the exponential decay model.

*Variable Size.* Experimentally, variation in quantal size arises in several ways. First, the same synaptic or generator current has decreasing effects the greater its distance from the site of impulse initiation. For a cable with a linear current-voltage curve, the effect of a maintained current decreases exponentially with distance (Hodgkin and Rushton, 1946). More complex geometries have also been considered (Rall, 1960; Noble, 1966). Secondly, the size of individual synaptic inputs varies with the very different areas of contact of different presynaptic fibers and the statistical fluctuations in transmitter release (Katz and Miledi, 1963).

Thirdly, the permeability changes may be specific for different ions (inhibitory or excitatory). Finally, when the variability is largely due to the opening and closing of single pores, the quantal duration is probably also random. Fig. 1C shows examples of long and short quantal current inputs with the corresponding voltage changes. If the mean quantal duration is much less than the time constant $\tau$, an exponential density of durations will produce a roughly exponential density of

TABLE I

ASSUMPTIONS OF THE QUANTAL MODELS CONSIDERED IN TEXT

Excitatory inputs occur at random times with mean rate $p_e$. The current-voltage curves of models 1–4 are assumed linear with a sharply defined threshold voltage. Threshold changes plus afterpotentials are included in a function $r(t)$. Further explanation in text.

| Model | Quantal effect | Subthreshold decay between inputs | Change upon reaching threshold |
|---|---|---|---|
| 1. Exponential decay | Unit voltage change | Exponential with time constant $\tau$ | Voltage reset |
| 2. Variable duration | Unit voltage change | At discrete times; duration of unit voltage changes variable with mean $\tau$ | Voltage reset |
| 3. Variable size | Voltage change having amplitude density function $q(a)$ with unit mean and variance $\sigma_a^2$ | Either model 1 or 2 above | Voltage reset |
| 4. Single pore | Unit current change | Current decay at discrete times; duration of unit current changes random with mean $t_p$; voltage changes exponential with time constant $\tau$ | Voltage reset; current unaffected |
| 5. Modified Hodgkin-Huxley | Unit current change | Current decay as in model 4 above with mean 1 msec; voltage changes according to Hodgkin-Huxley equations | Voltage changes according to Hodgkin-Huxley equations; current unaffected |

sizes (though with a limited maximum size). A mean duration much longer than the time constant will produce approximately rectangular voltage changes with constant size and variable duration similar to those of the variable duration model, though with important differences (see section on Single Pores).

What will be the effect on the nerve impulse pattern of these sources of variability in quantal size? Before answering this question in detail, I shall turn to a much more general consideration of voltage fluctuations in the absence of neuronal action potentials.

*Voltage Fluctuations.* Rice (1945) and others developed methods for analyzing the "shot noise" that results from the random emission of electrons in vacuum tubes, and much of this analysis is directly applicable to the voltage fluctuations of quantal models. I shall consider transient as well as steady-state phenom-

TABLE II

COMPARISON OF RESULTS FROM FOUR QUANTAL MODELS

Explanation of notation in text. Most of the results for the exponential decay model were derived by Stein (1965), for the variable duration model by Palm (1943) and the others are considered in the text. Equation (1.18) or (1.19) applies depending whether variability in size is added to the exponential decay or the variable duration model respectively. The formulae for $\mu \ll \tau$ in the variable size model were calculated assuming an exponential distribution of sizes. No refractory periods were included. Coefficients of variation greater than one and more than one exponential segment may arise in the variable size model when $t_p > \tau$. Equations (2.3) and (2.4) assume $t_p \gg \tau$.

| | 1. Exponential decay | 2. Variable duration | 3. Variable size | 4. Single pore |
|---|---|---|---|---|
| Mean voltage ($\mu_v$) | $p_e\tau(1 - e^{-t/\tau})$ | $p_e\tau(1 - e^{-t/\tau})$ | $p_e\tau(1 - e^{-t/\tau})$ | $p_e t_p(1 - e^{-t/\tau})$ |
| Variance ($\sigma_v^2$) | $(p_e\tau/2)(1 - e^{-2t/\tau})$ | $p_e\tau(1 - e^{-t/\tau})$ | Equation (1.18) or (1.19) | $\frac{(p_e t_p^2)(1 - e^{-2t/\tau})}{(t_p + \tau)}$ |
| Autocorrelation $\rho(h)$ | $e^{-h/\tau}$ | $e^{-h/\tau}$ | $e^{-h/\tau}$ | $\frac{t_p e^{-h/t}p - \tau e^{-h/\tau}}{t_p - \tau}$ |
| Mean interval, $\mu$ if $\mu \ll \tau$ | $r/p_e$ | $r/p_e$ | $(r + 1)/p_e$ | Equation (2.3) |
| Variance, $\sigma^2$ if $\mu \ll \tau$ | $r/p_e^2$ | $r/p_e^2$ | $(2r + 1)/p_e^2$ | Equation (2.4) |
| Coefficient of variation, $\sigma/\mu$, if $\mu \ll \tau$ | $r^{-0.5}$ | $r^{-0.5}$ | $\sqrt{2r + 1}/(r + 1)$ | $\sqrt{\mu/r\tau}$ |
| Interval density function, $f(t)$ if $\mu \ll \tau$ | Gamma $(r, p_e)$ | Gamma $(r, p_e)$ | Equation (1.35) | Normal |
| Coefficient of variation, $\sigma/\mu$, if $\mu \gg \tau$ | 1 | 1 | 1 | $\geq 1$ |
| Interval density function, if $\mu \gg \tau$ | Exponential | Exponential | Exponential | One or two exponential segments |

ena and calculate results for the models of previous sections. Let $g(u)$ be the voltage produced at a time $u$ after the occurrence of a quantal input. The total voltage $V(t)$ at time $t$ after the last nerve impulse will be a random variable and will equal the sum of the voltages produced by individual quanta so

$$V(t) = \int_0^t g(t - y)\, dN(y). \tag{1.11}$$

In a discrete approximation $\Delta N(y)$ would be the number of inputs occurring between times $y$ and $y + \Delta y$, and $V(t)$ is thus the weighted sum of a large number of random variables. For a Poisson process with mean input rate $p_e$ the variables are also independent with mean $p_e\Delta y$ and variance $p_e(\Delta y)^2$. From the properties of sums of independent random variables, the mean and variance in voltage as a function of time are

$$\mu_v = p_e \int_0^t g(t - y)\, dy = p_e \int_0^t g(u)\, du \tag{1.12}$$

$$\sigma_v^2 = p_e \int_0^t g^2(t - y)\, dy = p_e \int_0^t g^2(u)\, du. \tag{1.13}$$

Similarly the autocovariance function (Cox and Miller, 1965) is

$$\gamma_v(h) = p_e \int_0^{t-h} g(u)g(u + h)\, du \tag{1.14}$$

where

$$\gamma_v(0) = \sigma_v^2.$$

The autocorrelation function will be defined as the ratio $\rho_v(h) = \gamma_v(h)/\gamma_v(0)$ as $t \to \infty$ (Cox and Miller, 1965, p. 276) though electrical engineers (Middleton, 1960) use somewhat different definitions. For the exponential decay model $g(u) = \exp(-u/\tau)$; $\mu_v$, $\sigma_v^2$, and $\rho_v(h)$ are easily calculable and are listed in Table II. $\mu_v$ and $\sigma_v^2$ can be calculated using a different method (Stein, 1965; see also Moyal, 1949, p. 190), and Keilson and Mermin (1959) gave a further statistical description, but the more general equations (1.12) to (1.14) apply to any shaped input. Only if there is exponential decay will $\mu_v$ increase exponentially. For $t \to \infty$, equations (1.12) and (1.13) are known as Campbell's theorem. Rice (1945) generalized Campbell's theorem to an arbitrary density of quantal sizes assuming that the shape was independent of amplitude.

I shall denote the density function of amplitudes $q(a)$ and consider negative (inhibitory) as well as positive (excitatory) quanta. The total rate of quantal inputs will then be denoted $p$ without a subscript. If the mean amplitude is $\mathbf{a}$ and the second moment about the origin is $\mathbf{a}^2$, then it follows directly from Rice's work that the mean level is

$$\mu_v = p\mathbf{a} \int_0^t g(u)\, du \tag{1.15}$$

and the variance is

$$\sigma_v^2 = p\mathbf{a}^2 \int_0^t g^2(u)\, du. \tag{1.16}$$

Higher moments can also be calculated as desired.

If the mean amplitude is unity, equation (1.15) reduces to (1.12) but the variance in level will be increased since from the well-known relation between the second moments about the origin and about the mean, $\mathbf{a}^2 = 1 + \sigma_a^2$, where $\sigma_a^2$ is the variance in quantal amplitude. For the exponential decay model with added vari-

ability but unit mean quantal size

$$\mu_v = p_e\tau(1 - e^{-t/\tau}) \tag{1.17}$$

independent of the variability, and

$$\sigma_v^2 = (p_e\tau/2)(1 - e^{-2t/\tau})(1 + \sigma_a^2). \tag{1.18}$$

It follows from the definition of the autocorrelation function that it will not be affected by variability in quantal size. Cox and Miller (1965, section 9.6) further generalized equations (1.15) and (1.16) to any number of arbitrarily shaped populations and the results for the variable duration model (Table II) follow easily from their analysis. If variability is added but the mean remains one, equation (1.17) again holds, while the variance in level is

$$\sigma_v^2 = p_e\tau(1 - e^{-t/\tau})(1 + \sigma_a^2). \tag{1.19}$$

When $t \ll \tau$, both equations (1.18) and (1.19) reduce to

$$\sigma_v^2 = p_e t(1 + \sigma_a^2). \tag{1.20}$$

*Interval Distributions Assuming Negligible Decay.* From consideration of the fluctuations of voltage in the absence of a threshold, I shall now return to the fluctuations in time to reach a constant threshold. The interval density function can be calculated for short mean intervals with an arbitrary density of quantal sizes $q(a)$, as long as decay is negligible ($\mu \ll \tau$). Let $b_n(t)$ be the distribution of times to the $n$th input event. If the size of the $k$th event is $A_k$ and a random variable $V_n = A_1 + A_2 + \cdots + A_n$ is introduced for the total voltage produced by $n$ quanta, then a probability distribution function $Q_n(v) = \text{prob}\,(V_n \leq v)$ can be defined. For $t \ll \tau$ (before decay is appreciable) the interval density function $f(t)$ for a threshold $r$ is given by

$$f(t) = \sum_{n=1}^{\infty} b_n(t)[Q_{n-1}(r) - Q_n(r)] \tag{1.21}$$

where $Q_0(r) = 1$; $0 \leq t \leq \infty$. The expression in the brackets is the probability that the $n$th event causes the voltage to surpass $r$ for the first time. With negligible decay and Poisson inputs, $b_n(t)$ is the density function of a gamma distribution whose first two moments about the origin are $n/p$ and $(n + n^2)/p^2$. Thus,

$$\mu = \int_0^{\infty} tf(t)\,dt = \sum_{n=1}^{\infty} [Q_{n-1}(r) - Q_n(r)]\left[\int_0^{\infty} tb_n(t)\,dt\right]$$

$$= \frac{1}{p}\sum_{n=1}^{\infty} n[Q_{n-1}(r) - Q_n(r)]$$

$$\mu = \frac{1}{p}\sum_{n=0}^{\infty} Q_n(r) \tag{1.22}$$

and

$$\sigma^2 = \int_0^\infty t^2 f(t)\,dt - \mu^2 = \sum_{n=1}^{\infty} [Q_{n-1}(r) - Q_n(r)] \left[ \int_0^\infty t^2 b_n(t)\,dt \right] - \mu^2$$

$$= \frac{1}{p^2} \sum_{n=0}^{\infty} [n + 1 + (n+1)^2 - n - n^2] Q_n(r) - \mu^2$$

$$\sigma^2 = (2/p^2) \sum_{n=0}^{\infty} (n+1) Q_n(r) - \mu^2 \tag{1.23}$$

With negligible decay, this is a random walk model, though of a much more general kind than that considered by Gerstein and Mandelbrot (1964) since the size and time distribution of steps are random variables with an arbitrary distribution. Cox and Miller (1965) showed that the moments of the interval distribution are finite [and hence the sums of equations (1.22) and (1.23) converge] as long as the mean quantal size **a** is greater than zero. For **a** less than zero (predominant inhibition) the assumption of negligible decay must break down and the moments are then still finite (Stein, 1965).

Equation (1.21) is also valid for non-Poisson inputs, e.g., where the occurrence of a quantum increases or decreases the probability of a second quantum for a period of time. If the time $u$ to release of the next quantum is independently and identically distributed (renewal process, Cox, 1962) with density function $b(u)$ having mean $1/p$ and variance $\sigma_p^2$, then equation (1.22) for the mean interval still holds and the variance in interval becomes

$$\sigma^2 = (2/p^2) \sum_{n=1}^{\infty} n Q_n(r) + (\mu/p)(1 + \sigma_p^2 p^2) - \mu^2. \tag{1.24}$$

Laplace transforms are useful in evaluating the sums and transformed variables will be indicated by an asterisk. Taking the Laplace transform with respect to $t$ of the interval density function of equation (1.21)

$$f^*(s) = \sum_{n=1}^{\infty} [b^*(s)]^n [Q_{n-1}(r) - Q_n(r)]$$

where $b_n^*(s) = \int_0^\infty e^{-st} b_n(t)\,dt = [b^*(s)]^n$ if the times of quantal inputs are assumed to be identically and independently distributed (Cox, 1962) with density function $b(u)$ and Laplace transform $b^*(s)$. Then,

$$f^*(s) = b^*(s) Q_0(r) + [b^*(s) - 1] \sum_{n=1}^{\infty} [b^*(s)]^n Q_n(r) \tag{1.25}$$

and taking transforms again, this time with respect to $r$,

$$f^{**}(s) = \frac{b^*(s)}{\theta} + \frac{b^*(s) - 1}{\theta} \sum_{n=1}^{\infty} [b^*(s)]^n [q^*(\theta)]^n \tag{1.26}$$

where $Q_n^*(\theta) \equiv \int_0^\infty \exp(-\theta r) Q_n(r)\, dr = [q^*(\theta)]^n/\theta$ from the definition of $Q_n(r)$ as the cumulative probability that the sum of $n$ independent random variables [with density function $q(a)$ and transform $q^*(\theta)$] is less than $r$.

(If inhibitory quanta are considered, the integral defining $Q_n^*(\theta)$ must run from $-\infty$ to $+\infty$ and the Laplace transform is replaced by a Fourier transform.)

Equation (1.26) simplifies to

$$f^{**}(s) = \frac{b^*(s)[1 - q^*(\theta)]}{\theta[1 - b^*(s)q^*(\theta)]}. \tag{1.27}$$

For a Poisson process with rate $p$, $b(u) = p \exp(-pu)$ and $b^*(s) = p/(s + p)$. Equation (1.27) then becomes

$$f^{**}(s) = \frac{p[1 - q^*(\theta)]}{\theta[s + p - pq^*(\theta)]}$$

with inverse transform

$$f^*(t) = [p/\theta][1 - q^*(\theta)] \exp\{-pt[1 - q^*(\theta)]\}. \tag{1.28}$$

This is of the form $(x/\theta) \exp(-xt)$ which has a mean $(x\theta)^{-1}$ and second moment about the origin $2/(x^2\theta)$ from which it follows that

$$\mu^* = \{p\theta[1 - q^*(\theta)]\}^{-1} \tag{1.29}$$

$$(\sigma^2)^* = \frac{2}{p^2\theta[1 - q^*(\theta)]^2} - (\mu^2)^*. \tag{1.30}$$

These last expressions can also be obtained by transforming equations (1.22) and (1.23) so equation (1.29) holds independently of $b(u)$. Equation (1.24) would become

$$(\sigma^2)^* = \frac{2q^*(\theta)}{p^2\theta[1 - q^*(\theta)]^2} + \frac{\mu^*(1 + \sigma_p^2 p^2)}{p} - (\mu^2)^*. \tag{1.31}$$

Thus, when the quantal size varies but the mean interval is short, the interval density function, the mean, and the variance can be calculated from equation (1.21) to (1.24). Equations (1.27) to (1.31) give the Laplace transforms of these quantities in terms of the Laplace transform of the density function of quantal sizes and input times. The expressions for a Poisson process are easier to evaluate and will be illustrated by a couple of examples.

*Exponential Density of Quantal Sizes.* Assume that the density of quantal sizes is an exponential and that inhibition does not occur. In other words, assume

$$q(a) = e^{-a} \quad a \geq 0$$
$$= 0 \quad a < 0$$

which has a mean of one, a variance of one, and a Laplace transform $1/(1 + \theta)$. Then, from equation (1.29)

$$\mu^* = (1 + \theta)/(p_e\theta^2)$$

and the inverse transform gives

$$\mu = (r + 1)/p_e . \tag{1.32}$$

Comparing equation (1.32) with the corresponding formulas for no variaton in quantal size, Table II indicates that introducing an exponential density of quantal sizes increases the mean interval by $1/p_e$. Similarly, from equation (1.30)

$$(\sigma^2)^* = 2(1 + \theta)/(p_e^2\theta^3) + 2\mu^*/p_e - (\mu^2)^*$$

with inverse transform

$$\sigma^2 = r(r + 2)/p_e^2 + 2\mu/p_e - \mu^2 = (2r + 1)/p_e^2. \tag{1.33}$$

The coefficient of variation will therefore have the value

$$\sigma/\mu = (2r + 1)^{1/2}/(r + 1). \tag{1.34}$$

An extra source of variability generally increases the relative variability of the interval distribution and at large values of $r$, there is a constant factor increase of $\sqrt{2}$. Alternatively, the apparent quantal number is halved, since $r$ is replaced by $r/2$. However, the extra source of variability actually *decreases* the coefficient of variation when $r \leq 1.6$; the right-hand side of equation (1.34) does not approach one until $r \to 0$.

From equation (1.28) for the interval density function

$$f^*(t) = [p_e \exp(-p_e t)][(1 + \theta)^{-1} \exp\{p_e t/(1 + \theta)\}].$$

The inverse transform is (Hodgman, 1957, p. 320)

$$f(t) = p_e \exp(-p_e t - r) I_0(2\sqrt{p_e t r}) \tag{1.35}$$

where

$$I_0[2\sqrt{p_e t r}) = \sum_{n=0}^{\infty} (p_e t r)^n/(n!)^2$$

is a modified zero order Bessel function of the first kind.

*An Approximation Method.* Asymptotic result for large values of $r$ can be derived more easily by a useful approximate method. Fig. 4 indicates an average

growth of depolarization $v$ in the absence of neuronal firing. With a threshold level $r(t)$, the voltage distribution will project onto the time axis at the level $r(t)$ if three conditions are met: (*a*) the voltage distribution increases without spreading out or changing shape considerably near the level $r$; (*b*) there is not sufficient time for substantial redistribution to take place ($\sigma \ll \tau$); (*c*) $r(t)$ is nearly linear over the appropriate range of times (within a few standard deviation units of the mean interval). Then, the mean interval $\mu$ will occur at the time when $\mu_v = r(t)$ and one can write two equations for the standard deviation of the interval distribution from Fig. 4.

$$d\mu_v/dt = c/\sigma$$

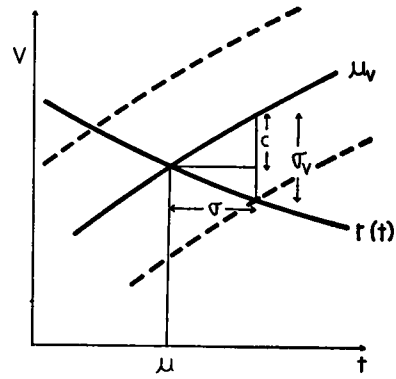


FIGURE 4 An approximation method for obtaining the mean ($\mu$) and standard deviation ($\sigma$) of the interval density function from the corresponding parameters ($\mu_v, \sigma_v$) of the voltage fluctuations in the absence of a threshold, $r(t)$. Applications and limitations of the method are discussed in the text. The voltage and time regions of interest are greatly magnified in the interests of clarity.

and

$$-dr(t)/dt = (\sigma_v - c)/\sigma.$$

Rearranging and eliminating the constant $c$, it follows that

$$\sigma = \sigma_v/(d\mu_v/dt - dr(t)/dt). \tag{1.40}$$

Time varying thresholds will be considered shortly (Refractoriness). If $r$ is constant, equation (1.40) reduces to

$$\sigma = \sigma_v/(d\mu_v/dt) \tag{1.41}$$

and conditions (a) and (b) listed above require that $r$ is large and $p_e\tau \gg r$, so the growth of depolarization (Table II) reduces to $\mu_v = p_e t$. Hence, $d\mu_v/dt = p_e$, $\mu = r/p_e$, and substituting from equations (1.20) and (1.41)

$$\sigma = \sqrt{r(1 + \sigma_a^2)}/p_e. \tag{1.42}$$

For large values of $r$ the interval distribution will be approximately normal so $\sigma$

and $\mu$ will completely specify the interval distribution. The coefficient of variation is

$$\sigma/\mu = \sqrt{(1 + \sigma_a^2)/r}. \tag{1.43}$$

For the exponential density considered above, $\sigma_a^2 = 1$ and equation (1.43) agrees with equation (1.34) for large values of $r$.

This approximation method is not limited to negligible decay. Equation (1.41) can be used, for example, to calculate $\sigma$ (and the coefficient of variation) for the exponential decay model, and the values agree well with computer simulated results if $\sigma < \tau/4$.

*Two Populations.* If two different quantal populations exist and say one-third of the quanta are of size 2.5 and the other two-thirds are 0.25, the mean size is one, the variance is 1.21, and the coefficient of variation for large $r$ from equation (1.43) is $(2.21/r)^{1/2}$. The coefficient of variation in the absence of the small quanta would be $(2.5/r)^{1/2}$ so the small quanta have little effect, though they are twice as abundant. Experimentally, only the largest amplitude population of quanta may warrant consideration.

*Refractoriness.* Varying the quantal size and duration in previous sections shifted the variability curve, but had relatively little effect on its shape. The addition of refractory periods changes the shape of the variability curve considerably. An absolute refractory period $t_0$ will simply shift a linear plot of $\sigma$ against $\mu$ to the right, but the coefficient of variation will be decreased, particularly at high stimulus strengths. If previously $\sigma/\mu$ approached a constant, $\sigma/(\mu + t_0)$ will approach zero. A relative refactory period will further decrease the variability as can be analyzed quantitatively from equation (1.40) if the function $r(t)$ is known. In the relative refractory period, $r(t)$ decreases with time so $dr(t)/dt$ is negative and $\sigma$ will be decreased. Thus, two of the assumptions on which the method was based, $\sigma \ll \tau$ and $r$ large, will hold over a wider range of conditions in the relative refractory period. However, $r(t)$ must be fairly linear over the region of interest.

### 2. *Longer Duration Inputs*

Previously I assumed that the quantal inputs were short-lasting and that the average number of quanta active at any one time was much less than threshold ($p_e t_p \ll r$). Release of a single packet of a long-lasting transmitter often produces a similarly shaped voltage change with a relatively short rising phase preceding a longer, nearly exponential decay as the transmitter is slowly inactivated or diffuses away. However, frequent long-lasting quantal inputs yield a different response. Voltage changes are much smoother (Fig. 1B) and an action potential will not normally affect the prolonged conductance changes producing the synaptic or generator currents. Indeed, a new nerve impulse may arise without any new quantal inputs. It is more convenient

to consider current changes here rather than voltage changes; the symbol $i$ will represent the number of quanta active relative to the peak current of a single input and $r$ will be the threshold number (rheobasic current) for maintained discharge.

*Intense Stimuli.* For a long conductance change, $t_p \gg \mu$, the current will be almost constant over a single interval and the interval density function $f(t)$ can be obtained from the frequency-current curve $\nu(i)$ by change of variables.

$$f(t)\,dt = y(i)w(i)\frac{dt}{di}\,di \tag{2.0}$$

where $y(i)$ is the density function of current strengths and $w(i)$ is a weighting factor needed because higher current strength produces more impulses in a given period of time. In other words, short intervals occur more often than otherwise predicted. $dt/di$ is the rate of change of interval with change in current.

Braitenberg (1965) described a related graphical method, but neglected to include a weighting factor. He also interpreted changes as threshold potential changes and neglected the local potential changes following an action potential which may be important.

The interval is the inverse of frequency so

$$t = 1/\nu(i)$$

$$dt/di = \frac{-d\nu(i)/di}{\nu^2(i)} \tag{2.1}$$

and

$$w(i) = M\nu(i)$$

where $M$ is a normalization factor chosen so that the integral of equation (2.0) over all $i$ is one. Then, equation (2.0) becomes

$$f(t)\,dt = -\frac{My(i)}{\nu(i)}\frac{d\nu(i)}{di}\,di. \tag{2.2}$$

The mean interval will be

$$\mu = -\int \frac{My(i)}{\nu^2(i)}\frac{d\nu(i)}{di}\,di \tag{2.3}$$

and the variance

$$\sigma^2 = -\int \frac{My(i)}{\nu^3(i)}\frac{d\nu(i)}{di}\,di - \mu^2. \tag{2.4}$$

$y(i)$ and $\nu(i)$ can be determined from experimental data or from a suitable model. Then, equations (2.3) and (2.4) can be integrated analytically or numerically, depending on the functions involved. For large $i$ and $t_p \gg \mu$, one can use graphical methods similar to those of Fig. 4 on a plot of the strength ($i$) against the duration ($t$) of a just-threshold stimulus (strength-duration) curve. Then,

$$di/dt = -\sigma_i/\sigma. \tag{2.5}$$

Under quite general conditions Noble and Stein (1966) showed that there is a constant charge relationship for strong stimuli ($i \gg r$), namely

$$it = \text{constant} = r\tau \tag{2.6}$$

where $r$ is the rheobasic number and $\tau$ the strength-duration time constant of the cell.

Noble and Stein's analysis assumed that the cells were quiescent, and is only strictly valid when refractory effects can be neglected. Qualitatively, refractoriness reduces the coefficient of variation at short mean intervals and will enhance the effect demonstrated below. Equation (2.5) should also include a weighting factor, but its effect will be secondary where variability is small.

Under these conditions it folllows from equation (2.6) that

$$\mu = r\tau/\mu_i \tag{2.7}$$

$$di/dt = -r\tau/t^2$$

and with equation (2.5)

$$\sigma = r\tau\sigma_i/\mu^2 = \sigma_i/(r\tau\mu_i^2) \tag{2.8}$$

$$\sigma/\mu = \sigma_i/\mu_i\,. \tag{2.9}$$

The ratio $\sigma_i/\mu_i$ can often be derived simply; rectangular quantal current inputs of random duration would yield a Poisson distribution of currents (analogous to the distribution of voltages in the variable duration model) with mean $p_e t_p$ and variance $p_e t_p$. If the current produced by single quantal inputs decayed exponentially, analogy with the exponential decay model would indicate that $\mu_i = p_e t_p$ and $\sigma_i^2 = p_e t_p/2$, i.e., half as large as above. For either model

$$\sigma/\mu = (bp_e t_p)^{-1/2} = (b\mu_i)^{-1/2} = (\mu/c)^{1/2} \tag{2.10}$$

where $b$ and $c$ are constants and $c = r\tau$ or $2r\tau$ respectively. Equation (2.10) demonstrates the important point that with increasing stimuli the coefficient of variation

continues to change as the square root of the mean interval, instead of approaching a constant value.

*Near-Threshold Stimuli.* The previous analysis assumed that the current strength was always well above threshold, and that the quantal durations were much longer than the mean interval. The interval distribution and its parameters were then determined from the frequency-current curve or the strength-duration curve. With weaker stimuli the current strength will drop below the threshold for generating a repetitive discharge during a substantial part of the time and the nerve cell will remain quiescent until the current again rises to a suprathreshold level. The interval density function will then show a "tail" of very long intervals. If correlations in membrane potential only extend over a finite period of time, then the interval density function will be approximately exponential at intervals long compared to the correlation time. As the stimulus strength is lowered, the "tail" comprises more and more of the interval density function until the function becomes entirely exponential and the coefficient of variation approaches one. However, the "two-part" density functions at intermediate values may have a standard deviation greater than the mean or a coefficient of variation greater than one. More quantitative results can be obtained with particular models.

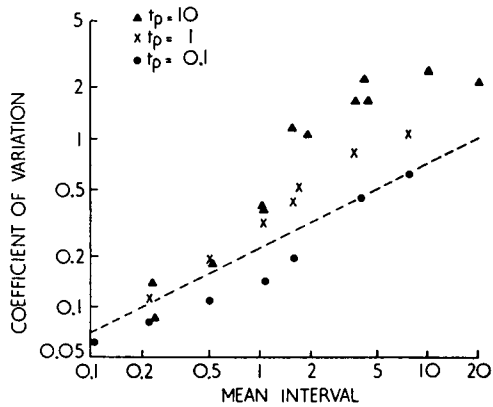


FIGURE 5 The effect of the mean quanta duration ($t_p$) on the variability curve. At short mean intervals the results approach the dashed line which represents the predictions of equation (2.10). The mean interval and mean quantal duration are in units of the time constant $\tau$; further explanation in text.

*Single Pores.* Table I lists the assumptions of the single pore model and Fig. 1C illustrates the current and voltage changes produced by the opening and closing of single permeability channels through the membrane. There are two independent time parameters: single pores stay open for a random time with mean $t_p$ while the voltage changes exponentially with a time constant $\tau$. Fig. 5 shows computer simulated variability curves for three different quantal durations ($t_p$ equal to $10\tau$, $\tau$, or $0.1\tau$) with the same rheobasic number ($r = 20$) of quantal currents. The variability at high intensities (short mean intervals) is proportional to the square root of the mean and approaches the prediction of equation (2.10). The coefficient

of variation for $t_p = 10\tau$ exceeds one at long mean intervals, also as predicted above. Finally, when $t_p = 0.1\tau$ and $t_p \ll \mu$, the predictions of the section on short-acting quanta are followed. To reach threshold requires on average $20 \times 10 = 200$ quantal *voltage* changes. The variable duration of open pores is evident as a variation in size and halves the apparent threshold number (see section on Variable Size). Thus, the variability curve is similar to that found for the exponential decay model with $r = 100$ (Fig. 3) as long as $\mu \gg t_p$, but for short mean intervals the variability continues to decrease according to equation (2.10).

Interval distributions with two approximately exponential regions (Fig. 6) are found near threshold when $t_p > \tau$. Although no refractory periods were included in the computations, virtually no impulses occurred for intervals less than $\tau$, due to the slow increase of voltage with near threshold stimuli. Between $\tau$ and $3\tau$ there is a

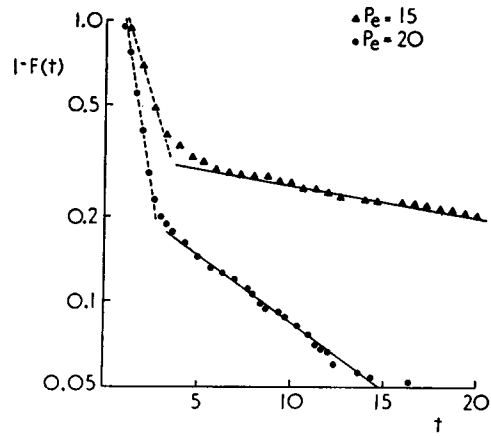


FIGURE 6 Interval distributions for near threshold stimuli. $1 - F(t)$ is the probability that the interval between two impulses is longer than $t$. On a semilog scale one can see that the distributions consist of two near-exponential segments. The "tail" (long interval segment) is much more sensitive to changes in input rate $p_e$ and represents an increasing fraction of the distribution as $p_e$ is lowered. $t_p = 10\tau$, and the values of $p_e$ represent the average number of inputs in a time $t_p$.

region (on a semilog scale) of high slope when the common suprathreshold values of current cause the voltage to reach threshold. If the current drops below the rheobasic value, threshold is not reached until the current again rises above rheobase. This time depends very critically on the value of $p_e$. Decreasing $p_e$ from 20 to 15 per $t_p$ increased the time constant of the tail of the density function (as determined from the slope of the solid lines in Fig. 6) from $9\tau$ to $37\tau$.

In the single pore model, current fluctuates with mean $t_p$ in the same way as voltage does in the variable duration model with mean $\tau$. If current drops to the rheobasic level $r$, excitation would take an infinitely long time. In fact the current will fluctuate and one can calculate the mean time ($\mu_{r+1}$) for the level to rise again to $r + 1$ and so estimate the "time constant of the tail" of the interval density function. From equation (1.1)

$$f^*_{r,r+1}(s) = p_e B_r(s)/B_{r+1}(s) \tag{2.11}$$

and

$$\mu_{r+1} = -\left.\frac{\partial f^*_{r,r+1}(s)}{\partial s}\right|_{s=0} = p_e \frac{[B'_{r+1}(0)B_r(0) - B_{r+1}(0)B_r'(0)]}{[B_{r+1}(0)]^2}$$

where as before $Q_k(0) = p_e^k$, $Q_k'(0) = \sum_{j=0}^{k-1} (k!/j!)(p_e^j/(k-j))$. After some algebra, one finds

$$\mu_{r+1} = (r!/p_e^{r+1}) \sum_{j=0}^{r} p_e^j/j! \tag{2.12}$$
$$\sim (r/p_e)^{r+1}\sqrt{2\pi/r}\exp(p_e/r).$$

$\mu_{r+1}$ in equation (2.12) is in units of $t_p$, and $p_e$ in terms of events/$t_p$. To convert to other units, one must multiply by the value of $t_p$. The approximation follows from substituting Stirling's formula for factorials and noting that the sum in equation (2.12) is the first $r + 1$ terms for the power series expansion of exp $(p_e)$.

The fractional error in Stirling's formula is less than $(12r - 1)^{-1}$ which for $r = 20$ is less than 0.5%. However, for $p_e$ greater than or about equal to $r$, higher order terms in the expansion of exp $(p_e)$ may cause substantial errors.

The values of $\mu_{r+1}$ calculated from equation (2.12) are $3.15\tau$ and $14.6\tau$ for $p_e$ equal to 20 and 15 per $t_p$ respectively and they underestimate the values measured above from computer simulations. This will generally be true since there remains the probability that the current will not remain at $r + 1$ long enough for excitation to occur, but the simulated values would approach those calculated from equation (2.12) if $t_p$ were further increased.

*Current Changes and Voltage Changes.* For a linear circuit, the transfer function, or its inverse Laplace transform, the impulsive response (Schwartz, 1963) specifies the relation between current and voltage. In the simple linear membrane considered so far, the applied current $I(t)$ is divided between a capacitative and an ionic current

$$I(t) = C\,dV(t)/dt + V(t)/R \tag{2.21}$$

where $C$ is the membrane capacity and $R$ the membrane resistance. Taking Laplace transforms,

$$I^*(s) = V^*(s)[1 + s\tau]/R \tag{2.22}$$

where $\tau = RC$. The transfer function $L^*(s)$ is then

$$L^*(s) \equiv V^*(s)/I^*(s) = R/[1 + s\tau] \tag{2.23}$$

and the impulsive response $L(t) = (1/C)\exp(-t/\tau)$. The voltage is then obtained

from the superposition integral

$$V(t) = \int_0^t L(y)I(t - y)\, dy. \tag{2.24}$$

To derive the mean and other statistics of $V(t)$, consider the expected values or ensemble average (denoted $E\{X\}$ where $X$ is a random variable) produced by a fluctuating current applied a large number of times for a duration $t$.

$$\begin{aligned} \mu_v(t) = E\{V(t)\} &= E\left\{\int_0^t L(y)I(t - y)\, dy\right\} \\ &= \int_0^t L(y)\, dy\, E\{I(t - y)\} = \mu_i \int_0^t L(y)\, dy. \end{aligned} \tag{2.25}$$

Also,

$$\begin{aligned} \sigma_v^2(t) &= E\{[V(t) - \mu_v(t)]^2\} = E\left\{\left(\int_0^t L(y)[I(t - y) - \mu_i]\, dy\right)^2\right\} \\ &= \int_0^t \int_0^t L(y)L(z)\, dy\, dz\, E\{[I(t - y) - \mu_i]\,[I(t - z) - \mu_i]\} \\ \sigma_v^2(t) &= \int_0^t \int_0^t L(y)L(z)\gamma_i(y - z)\, dy\, dz \end{aligned} \tag{2.26}$$

where the last step follows from or serves as a definition of an autocovariance function for applied current. Similarly the steady-state voltage autocovariance function will be

$$\gamma_v(h) = \int_0^\infty \int_0^\infty L(y)L(z)\gamma_i(y + h - z)\, dy\, dz \tag{2.27}$$

and the autocorrelation function $\rho_v(h) = \gamma_v(h)/\gamma_v(0)$. Voltage changes were assumed not to affect the current in the single pore model and thus the current levels at all times are distributed according to a Poisson distribution (Palm, 1943) with mean and variance both $p_e t_p$ and autocorrelation function $\exp(-|h|/t_p)$. The absolute value sign is included in the last expression because $h$ may have negative values. The expressions for $\mu_v$, $\sigma_v^2$, and $\rho_v(h)$ listed in Table II for the single pore model follow from equations (2.25) and (2.27). However, these expressions will not be exact when there is strong correlation between successive intervals, because intervals will begin more often when $I(t)$ is high while the expected values assume random sampling of $I(t)$.

*Excitatory and Inhibitory Conductance Changes.* In practice, the ionic currents will depend on voltage, although the conductances (or permeabilities) may

not. If both excitatory, $G_e(t)$, and inhibitory, $G_i(t)$, permeability changes are present and vary as a function of time, but not voltage, equation (2.21) becomes

$$C\,dV(t)/dt + G_0V(t) + G_e(t)[V(t) - V_e] + G_i(t)[V(t) - V_i] = 0 \quad (2.28)$$

where the following are constants: $V_e$, the excitatory equilibrium potential; $V_i$, the inhibitory equilibrium potential; and $G_0$, the resting membrane conductance. Equation (2.28) is still a linear differential equation whose general solution is known (see for example Sokolnikoff and Redheffer, 1958, section 1.10). However, the statistics of $V(t)$ are not easily calculable in closed form.

*Point-Polarized Cable.* Finally, consider a nerve fiber stimulated at one point. An extra term must be added to equation (2.21) to account for the spread of current and if the fiber approximates to a linear electrical cable, the well-known equation (2.31) results (Hodgkin and Rushton, 1946; Noble and Stein, 1966).

$$\delta(x)I(t) = C\partial V(x, t)/\partial t + V(x, t)/R - K\partial^2V(x, t)/\partial x^2 \quad (2.31)$$

where $x$ is the distance along the cable and the point nature of the stimulus is specified by $\delta(x)$, the Dirac delta function. $K$ is a constant depending on the cable diameter and the axoplasmic resistivity. Taking Laplace transforms over $t$,

$$\delta(x)RI^*(s) = (1 + s\tau)V^*(x, s) - \lambda^2\partial^2V^*(x, s)/\partial x^2 \quad (2.32)$$

where $\tau = RC$ and $\lambda = \sqrt{RK}$ is the length constant of the fiber. At points other than $x = 0$, equation (2.32) is a homogeneous partial differential with solution

$$V^*(x, s) = A^* \exp(-\sqrt{1 + s\tau}\, x/\lambda)$$

and from the boundary condition at $x = 0$, it can be shown (Noble and Stein, 1966) that $A^* \propto I^*(s)/\sqrt{1 + s\tau}$. (For the remaining results of this section I shall only be concerned with the functional form of the relationships, so that constant factors will not be important.) Then the transfer function is

$$L^*(s) \equiv V^*(s)/I^*(s) \propto \exp[-\sqrt{1 + s\tau}\, x/\lambda]/\sqrt{1 + s\tau} \quad (2.33)$$

and the impulsive response (see also Noble and Stein, 1966, equation A13)

$$L(t) \propto (t/\tau)^{-0.5} \exp[-(x/\lambda)^2/(4t/\tau) - t/\tau]. \quad (2.34)$$

By inserting (2.34) into (2.25) to (2.27) one can obtain the statistics of the voltage fluctuations as a function of distance, but the more complicated form of equation (2.34) makes analytical solutions much more difficult. However, certain results follow immediately. According to the Wiener-Khintchine theorem, the power spectrum and the autocorrelation function are a Fourier transform pair. An exponential

autocorrelation function with time constant $\tau$ leads to a power spectrum, $P(\omega)$, which falls off at high sinusoidal frequencies, $\omega$, as $1/\omega^2$.

$$P(\omega) = \frac{\tau^2}{\tau^2 + \omega^2}. \tag{2.35}$$

If the input current and the output voltage are related by a transfer function $L^*(s)$, the power spectrum of voltage fluctuations is (Schwartz, 1963)

$$P_v(\omega) = |L^*(j\omega)|^2 P_i(\omega) \tag{2.36}$$

where $j$ is the square root of $-1$. At the origin the power spectrum of the current will be multiplied by a factor $[1 + (\omega\tau)^2]^{-0.5}$ and in the range $1/\tau \ll 2\pi\omega \ll 1/t_p$, the power spectrum will decrease as $1/\omega$. Away from the origin the power spectrum will decrease much more rapidly because of the exponential in equation (2.33). If one integrates over the entire cable (either to consider total charge movements or because the current sources may be distributed uniformly over the length of the cable), equation (2.33) reduces to the same form as equation (2.23) and the spectrum will contain a factor equal to the right-hand side of equation (2.35). The presence of a region where the power spectrum may fall as $1/\omega$ is of interest because of the experimental results of Verveen and Derksen (1965), Derksen (1965), and Derksen and Verveen (1966). There are, however, important differences that must be taken into account in interpreting the experimental data. First, Verveen and Derksen experimented on a nodal membrane whose properties are different from the linear cable. Secondly, the $1/\omega$ region began at $\omega \sim 0.0001/\tau$ if $\tau$ is the membrane time constant which is a much lower frequency than predicted here. Thirdly, the effects of the three terminal recording arrangement with feedback isolation (Derksen, 1965) must be taken into account.

### *3. Hodgkin-Huxley Equations*

The Hodgkin-Huxley equations (Hodgkin and Huxley, 1952) contain a much more complete and complicated description of neuronal activity than the models considered previously. A number of oscillatory systems are contained in their formulation and by suitably altering parameters, Lewis (1965) produced a wide variety of interval density functions (exponential, multimodal) from interactions among these systems even without a variable input source. However, with the standard constants of the Hodgkin-Huxley equations an applied current produces a completely regular train of nerve impulses (Fitzhugh and Antosiewicz, 1959) and a source of variability must be introduced to obtain variation in successive intervals. For comparison with simpler models the stimulus current was assumed to change randomly by unit amounts as in the single pore model (Table I). The rheobasic number ($r$) of quantal current changes was again 20 and the mean duration ($t_p$) was 1 msec. Noble and

Stein (1966) calculated a "strength-duration time constant" of 2.9 msec for the Hodgkin-Huxley membrane equations and gave details of the equations and computing methods (see also Fitzhugh and Antosiewicz, 1959, and Cooley, Dodge, and Cohen, 1965).

*Input-Output Relation.* With a constant applied current there are definite minimum and maximum impulse frequencies for the Hodgkin-Huxley equations (Stein, 1967). The minimum impulse frequency at 6.3°C is surprisingly high (>50 impulses/sec) and rather resistant to some simple changes of parameters. This results from the strong accommodation of the Hodgkin-Huxley equations and its dual nature; a constant current must excite in a rather short time if Na inactivation and K activation are not to prevent excitation. With an added source of variability, the

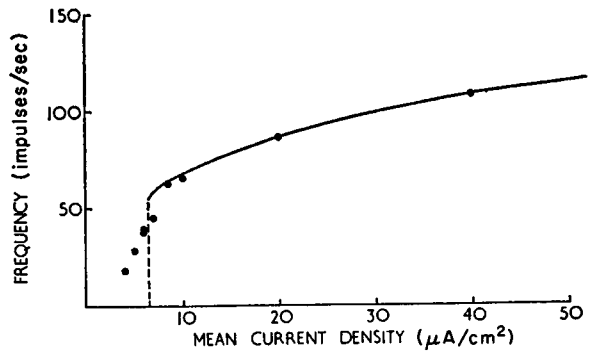


FIGURE 7 Input-output relation for Hodgkin-Huxley equations without variability (lines) and with a fluctuating current source (data points). In the absence of variability the maintained frequency changes discontinuously from 0 to over 50 impulses/sec (dashed vertical line) at about 6.5 $\mu$A/cm$^2$.

minimum steady frequency is no longer apparent in the input-output relation (Fig. 7). Near the rheobasic value for a constant current, however, the mean frequency is substantially reduced because the current may drop to subthreshold values temporarily and produce much longer intervals. Similar results apply to the conducted action potentials (Stein, 1967) obtained when the membrane equations are solved together with the equations for spread of voltage along a cable (Hodgkin and Rushton, 1946).

*Interval Distributions.* When the mean stimulus strength is high, there is relatively little variability in interval and the interval distribution is approximately normal (see Fig. 8A which uses graph paper designed so that a normal distribution plots as a straight line). With near threshold stimuli (Fig. 8B) a more complex curve results. In Fig. 8B, as in Fig. 6, log [1 − $F(t)$] has been plotted as a function of time since the conditional probability function, $\varphi(t)$, is proportional to the slope on this plot (as explained under Notation). For the first 15 msec few impulses occur, but

from 15 to 20 msec the conditional probability is high. From 20 to 30 msec $\varphi(t)$ is again low, but rises to a roughly constant value after 30 msec. Significantly, the transition from high to low conditional probability occurs at about the interval corresponding to the minimum firing frequency with steady currents. Although the maintained discharge no longer cuts off sharply at a particular current strength, accommodation still affects the conditional probability function. The membrane voltage and excitability tend to show similar damped oscillations as long as no action potential is produced and experimentally the conditional probability function can provide a useful indirect measure of these excitability changes.

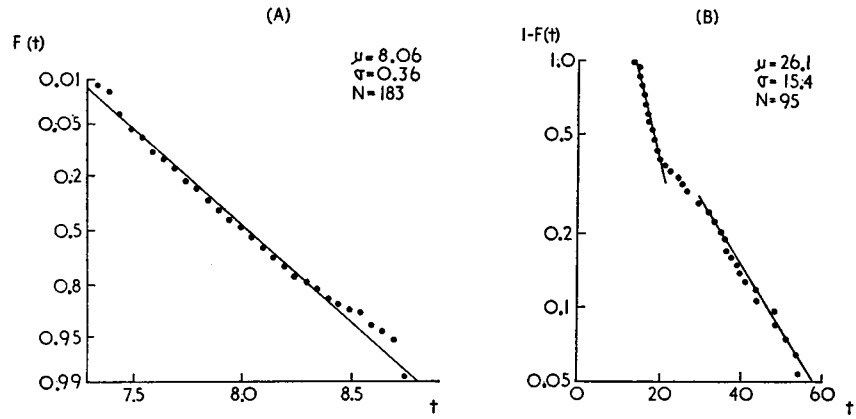


FIGURE 8 Interval distributions for Hodgkin-Huxley equations with strong (A) and weak (B) fluctuating current stimuli. In (A) the distribution is nearly normal as indicated by plotting the data points on graph paper constructed so that a normal distribution plots as a straight line. The solid line is the normal distribution with the sample mean and standard deviation. With weak stimuli (B) the distribution is more complex as indicated by plotting $\log [1 - F(t)]$ against time $t$. The slope on this plot is related to the conditional probability of firing at time $t$ if an impulse had not occurred before $t$.

*Coefficient of Variation.* The variability of this modified Hodgkin-Huxley model is plotted as a function of mean interval in Fig. 9 (filled circles). Although showing similarities to the variability of simpler models (Fig. 5), there are certain quantitative differences. Accommodation causes a sharper increase in variability at mean intervals around 20 msec while refractoriness reduces the variability at short mean intervals. A cable whose membrane properties obey the Hodgkin-Huxley equations cannot conduct two action potentials at 6.3°C unless separated by more than 5 msec (Stein, 1967). If 5 msec is subtracted from the mean interval as a refractory period, the variability curve (the open circles in Fig. 9) agrees more closely with those of simpler models (Figs. 3 and 6).

Although the threshold voltage is also increased at separations beyond 5 msec (relative refractory period) in the Hodgkin-Huxley equations, another factor opposes its effect on the variability curve. The maintained stimulus current prevents a full repolarization after an action potential, so depolarization begins again from a

potential nearer threshold. Indeed, with strong enough currents the membrane remains so depolarized that it becomes inactive and the discharge blocks.

*Serial Correlation.* An interesting difference between the Hodgkin-Huxley equations and the simpler models considered here is the dependence of one interval on the length of the previous interval. The current fluctuations of the single pore model have an autocorrelation $\exp(-t/t_p)$ and when $t_p$ is of the order of the

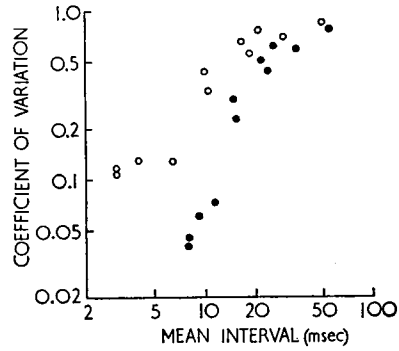


FIGURE 9 Relative variability as a function of mean interval for the Hodgkin-Huxley membrane equations with fluctuating currents. The open circles are obtained by applying a correction for refractory period to the original data (filled circles). Log-log scale.

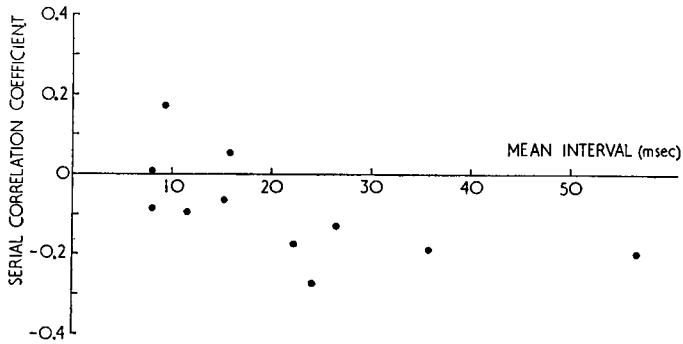


FIGURE 10 Correlation between successive intervals as a function of mean interval for the Hodgkin-Huxley membrane equations. At long means successive intervals tend to be negatively correlated.

neuronal impulse intervals, stimuli during successive intervals are positively correlated. However, with the Hodgkin-Huxley calculations and $t_p = 1$ msec, successive intervals tended to be *negatively* correlated at the longer intervals (Fig. 10). This is presumably due to accumulation of refractoriness if two action potentials are close together, so a longer than average interval tends to follow a shorter than average interval.

## DISCUSSION

Predictions for several models of neuronal variability have been derived, analytically where possible, or by computer simulation studies. The experimenter is often

interested in the opposite process of trying to infer from his data the models or mechanisms responsible and I shall try now to draw together some important results for this task. With no variability the relation between the rate of excitatory inputs and the mean nerve impulse frequency (input-output curve) may be fairly linear at middle frequencies, but negative deviations from linearity occur both at high and low frequencies. The addition of variability has little effect on the negative deviations at high frequencies due to refractoriness (Fig. 7), but greatly reduces or even reverses the negative deviations at low frequencies (Fig. 2). Accommodation or a supernormal period of increased excitability following a nerve impulse set a maximum interval (minimum frequency) for impulse initiation with constant currents (Stein, 1967). A source of variability removes this limit from the input-output curve, but the conditional probability function (see Notation) may still decrease sharply at this maximum interval (Fig. 8B).

The models considered here (Table I) all assume that variability arises from the random occurrence of quantal inputs. As a measure of relative variability, the coefficient of variation ($\sigma/\mu$) of the interval distribution was plotted against mean interval on a log-log scale. For the exponential decay model (Fig. 3) this "variability curve" shows three regions. At long mean intervals the coefficient of variation is one (exponential density function); at short mean intervals it is a constant which depends on the minimum number of quantal inputs needed to reach the threshold voltage. A transition region in which the rate of change of the coefficient of variation was also a function of the threshold number joins the two extremes. Variability in the size of quantal inputs decreases the apparent threshold number [see for example equation (1.34)] while variability in their duration mainly shifts the variability curve toward shorter mean intervals (Fig. 3). Refractoriness or the persistence of a long-acting transmitter will decrease the variability selectively at short mean intervals. Instead of approaching a constant, the variability will continue to fall as the mean interval is decreased (Fig. 5). With near threshold stimuli, the coefficient of variation tends to *exceed* one if the quantal duration is long. This was associated with an interval density function having two distinct, near-exponential regions, reminiscent of interval histograms found experimentally by Smith and Smith (1965). Although the model Smith and Smith proposed, in which switching occurred between two separate random processes, may be appropriate for cortical cells under their experimental conditions, other models with slowly fluctuating random inputs can produce a similar distribution.

A prolonged transmitter action will tend to produce positive correlations between successive intervals. Distributions with long "tails" can also be produced by membrane accommodation or inhibitory inputs (Stein, 1965) without the presence of positive serial correlations. Small negative serial correlations may be most easily explained by the negative feedback inherent in the Hodgkin-Huxley equations (Fig. 10). The oscillatory nature of these equations can produce more complex distributions with suitable modifications (Lewis, 1965) including multimodal distributions

such as those reported by Bishop, Levick, and Williams (1964) and others. Such distributions could also arise from a patterned input to the cell though this possibility might be distinguished by testing whether an interjected impulse resets the rhythm of the cell (Jansen, Nicolayson, and Rudjord, 1966).

Detailed comparison of the statistical properties of experimental data with the predictions of neuronal models such as discussed here can greatly narrow the range of possible mechanisms. A great deal of information can be obtained beyond that available from visual inspection of records or an interval histogram (see for example the recent paper of Hyvärinen, 1966) and a careful analysis may suggest further experiments to distinguish between the remaining possible mechanisms.

This investigation was supported in part by a U.S. Public Health Service Fellowship 1-FZ-GM-29, 201-01.

*Received for publication 30 September 1966.*

## REFERENCES

ADOLPH, A. R. 1964. *J. Gen. Physiol.* **48:** 297.
ADRIAN, E. O., AND Y. ZOTTERMAN. 1926. *J. Physiol., (London).* **61:** 151.
BARLOW, H. B. 1963. *Kybernetik.* **2:** 1.
BIEDERMAN-THORSON, M. 1966. *J. Gen. Physiol.* **49:** 597.
BISHOP, P. O., W. R. LEVICK, AND W. O. WILLIAMS. 1964. *J. Physiol., (London).* **170:** 598.
BRAITENBERG, V. 1965. *J. Theoret. Biol.* **8:** 419.
COOLEY, J., F. DODGE, AND H. COHEN. 1965. *J. Cell. Comp. Physiol., Suppl.* 2 **66:** 99.
COX, D. R. 1962. Renewal Theory. Methuen & Co. Ltd., London.
COX, D. R., AND H. D. MILLER. 1965. The Theory of Stochastic Processes. Methuen & Co. Ltd., London.
DERKSEN, H. E. 1965. *Acta Physiol. Pharmacol. Neerl.* **13:** 373.
DERKSEN, H. E., AND A. A. VERVEEN. 1966. *Science.* **151:** 1388.
FISZ, M. 1963. Probability Theory and Mathematical Statistics, 3rd edition, John Wiley & Sons, Inc., New York.
FITZHUGH, R., AND H. A. ANTOSIEWICZ. 1959. *J. Soc. Ind. Appl. Math.* **7:** 447.
GEISLER, C. D., AND J. M. GOLDBERG. 1966. *Biophys. J.* **6:** 53.
GERSTEIN, G. L., AND N. Y.-S. KIANG. 1960. *Biophys. J.* **1:** 15.
GERSTEIN, G. L., AND B. MANDELBROT. 1964. *Biophys. J.* **4:** 41.
GOLDBERG, J. M., H. O. ADRIAN, AND F. D. SMITH. 1964. *J. Neurophysiol.* **27:** 706.
HILL, A. V. 1936. *Proc. Roy. Soc. (London), Ser. B.* **119:** 305.
HODGKIN, A. L., AND A. F. HUXLEY. 1952. *J. Physiol.*, (London). **117:** 500.
HODGKIN, A. L., AND W. A. H. RUSHTON. 1946. *Proc. Roy. Soc. (London) Ser. B.* **133:** 444.
HODGMAN, C. D., editor 1957. Chemical Rubber Co. Standard Mathematical Tables, 11th edition. Chemical Rubber Co., Cleveland.
TEN HOOPEN, M. 1966. *Biophys. J.* **6:** 435.
HYVÄRINEN, J. 1966. *Acta Physiol. Scand.* **68:** (Suppl. 278).
ISO, Y. 1965 *In* Digest of the 6th International Conference on Medical Electronics and Biological Engineering, Tokyo.
JANSEN, J. K. S., K. NICOLAYSON, AND T. RUDJORD. 1966. *J. Physiol., (London).* **185:** 28P.
KATZ, B., AND R. MILEDI. 1963. *J. Physiol., (London).* **168:** 389.
KEILSON, J., AND N. D. MERMIN. 1959. *IRE Trans. Inform. Theory.* **5:** 75.
LEWIS, E. R. 1965. *J. Theoret. Biol.* **10:** 125.
MARTIN, A. R., AND G. PILAR. 1964. *J. Physiol., (London).* **175:** 1.
MIDDLETON, D. 1960. An Introduction to Statistical Communication Theory. McGraw-Hill Book Company, New York.

MOORE, G. P., D. H. PERKEL, AND J. P. SEGUNDO. 1965. *Ann. Rev. Physiol.* **28:** 493.
MOYAL, J. E. 1949. *J. Roy. Stat. Soc., London, Series B.* **11:** 150.
NOBLE, D. 1966. *Physiol. Rev.* **46:** 1.
NOBLE, D., AND R. B. STEIN. 1966. *J. Physiol., (London).* in press.
PALM, C. 1943. *Ericsson Technics.* **44:** 1.
POGGIO, G. F., AND L. J. VIERNSTEIN. 1964. *J. Neurophysiol.* **27:** 517.
RALL, W. 1960. *Exp. Neurol.* **2:** 503.
RICE, S. O. 1944. *Bell System Tech. J.* **23:** 282.
SCHWARTZ, L. S. 1963. Principles of Coding, Filtering and Information Theory, Spartan Books, Inc., Baltimore.
SILK, N., AND R. B. STEIN. 1966. *J. Physiol., (London).* **186:** 40P.
SMITH, D. R., AND G. K. SMITH. 1965. *Biophys. J.* **5:** 47.
SOKOLNIKOFF, I. S., AND R. M. REDHEFFER. 1958. Mathematics of Physics and Modern Engineering. McGraw-Hill Book Company, N. Y.
STEIN, R. B. 1965. *Biophys. J.* **5:** 173.
STEIN, R. B. 1967. *Proc. Roy. Soc. (London), Ser. B.* in press.
STEIN, R. B., AND P. B. C. MATTHEWS. 1965. *Nature.* **208:** 1217.
VERVEEN, A. A. 1962. *Acta Morphol. Neerl. Scand.* **5:** 79.
VERVEEN, A. A., AND H. E. DERKSEN. 1965. *Kybernetik.* **2:** 152.